ChemElectroChem

Research Article
doi.org/10.1002/celc.202500100

Chemistry Europe
European Chemical Societies Publishing

www.chemelectrochem.org

Electroenzymatic CO_2 Reduction Using Formate Dehydrogenase: Direct and Mediated Catalysis

Navendu Paul,* Isabel Moura, Luísa B. Maia, Cristina M. Cordas,* and Jose J. G. Moura*

The electrocatalytic reduction of carbon dioxide (CO_2) to formate by the enzyme formate dehydrogenase (FDH) makes use of the enzyme's observed reversibility, offering a promising strategy for the mitigation of CO_2 and the production of value-added compounds. To enhance the catalytic potential of *Desulfovibrio desulfuricans* FDH (*Dd*FDH), a range of artificial and natural redox cofactors is investigated using electrochemical methods. These studies included direct (nonmediated) conditions and mediated conditions employing viologens (methyl and benzyl viologens), and small heme proteins (cytochromes). Methyl viologen acts as an efficient mediator for CO_2 reduction, achieving a very high current density of 216 μA cm^{-2}. The studies of the different small proteins, namely cytochrome split-soret (*cyt* SS), cytochrome c_3 (*cyt* c_3), and cytochrome c_{552} (*cyt* c_{552}), allow the identification of the potential natural physiological partners. These isolated cytochromes, from the same organism, are electrochemically characterized, from which detailed redox processes are determined and later used as mediators to explore *Dd*FDH catalytic activity in both formate oxidation and CO_2 reduction. Best results are attained with cytochrome *cyt* SS and *cyt* c_3, increasing the electrocatalytic activity for formate oxidation by 7.5 times and 5.8 times, respectively.

1. Introduction

Atmospheric CO_2 mitigation has been considered crucial in addressing climate change issues,[1,2] not only lowering CO_2 concentrations but also enabling the potential use of CO_2 as an inexpensive and abundant resource for producing fuels and valuable chemical feedstocks.[3,4] In this context, electrochemical CO_2 reduction powered by a renewable energy source has been considered a promising approach, especially if achieved at ambient conditions, facilitating the catalytic reaction to occur.[5–7] Although significant advances have been made in developing synthetic electrocatalysts for CO_2 reduction, redox enzymes are recognized as highly efficient catalysts that can serve as a promising alternative due to their reversibility, unique product selectivity, low overpotential, mild experimental conditions, and fast catalytic rates.[8–11]

Metal-dependent formate dehydrogenases (FDHs)[12–14] are redox enzymes possessing the ability to catalyze the reversible two-electron conversion between CO_2 and formate (Equation (1)).

$$HCOO^- \rightleftharpoons CO_2 + H^+ + 2e^- \quad (1)$$

These enzymes, isolated from prokaryotic organisms, contain molybdenum (or tungsten) metal ions at the redox-active sites as well as multiple iron–sulfur [Fe–S] cofactors, which are responsible for an efficient wiring within the 3D protein subunits transferring electrons between the active site and the physiological redox partner.[12–14] This makes metal-dependent FDHs appropriate to be applied in a bioelectrochemical system (BES) either by direct electron transfer (DET) or by mediated electron transfer (MET) catalysis.[15] Other members of the formate dehydrogenase family group do not contain redox cofactors, being dependent on the NAD^+/NADH couple as redox partner.[16–18] There are reports with these metal-independent FDHs, some of which are commercially available, such as *Candida boidinii*,[19] showing mediated catalysis of CO_2 into formate. Electrochemical setups were designed to regenerate the natural cofactor, NADH, for wild-type[20–23] as well as mutant[24,25] metal-independent enzymes. However, this process requires an expensive NADH cofactor and imposition of high overpotentials.[26] Other methods have been developed to replace NADH as a cofactor[27] or to proceed one step further by catalyzing without any cofactor.[28] In contrast, metal-dependent FDHs from various sources can be directly attached to electrode surfaces (modified or unmodified, e.g., carbon) or encapsulated within conducting matrices and transfer electrons directly to the surfaces.[29–35] It can also be mediated with small artificial redox cofactors.[36–39] With these metal-dependent FDHs, immobilization in the proper orientation is essential to minimize the distance between the enzyme's redox cofactor(s) (the metal center) and the electron donor or acceptor, whether through MET via artificial or physiological compounds or DET to an electrode.[40]

Molybdenum-containing FDH from *Desulfovibrio desulfuricans* (*Dd*FDH) is well-suited for inclusion into BESs, as has been

N. Paul, I. Moura, L. B. Maia, C. M. Cordas, J. J. G. Moura
LAQV, REQUIMTE (Associated Laboratory for Green Chemistry)
NOVA School of Science and Technology
NOVA FCT
2829-516 Caparica, Portugal
E-mail: n.paul@fct.unl.pt
c.cordas@fct.unl.pt
jjgm@fct.unl.pt

Supporting information for this article is available on the WWW under https://doi.org/10.1002/celc.202500100

reported previously by our group, being one of the most efficient enzymes to reduce CO_2 with high substrate affinity and fast catalytic rate.[41,42] *Dd*FDH, found in the periplasm fraction, is a heterotrimeric complex redox enzyme with multiple cofactors having a molybdenum active site deeply buried within the protein structure, where the molybdenum ion is coordinated by four sulfur atoms from two pyranopterin moieties and in an oxidized state, it contains a terminal sulfo group along with a selenium atom from a selenocysteine residue. This enzyme also features two other types of redox-active centers, comprising four [4Fe–4S] clusters and four *c*-type hemes, constituting the electron transfer pathway.[8,43,44] Current reaction mechanism points that in the forward reaction of the catalytic cycle for formate oxidation, Mo^{VI} (=S) receives two electrons, as a hydride that is transferred from formate and similarly, in the reverse reaction, Mo^{IV}(—S—H) transfers the hydride ion to reduce CO_2 to formate and itself undergoes two-electron oxidation to generate the initial state.[41,45] These two electrons involved in the catalytic cycle are relayed through the internal cofactors to or from the specific physiological partner of *Dd*FDH. Depending upon this electron transfer reaction and the structure, the enzyme is expected to have preferential sites for the electronic pathway.[46] These sites may be accessed directly or through an external redox mediator, corresponding to direct or mediated electrochemical methods, respectively.[47] Preliminary electrochemical characterization with *Dd*FDH has also shown promising results. Reversible catalytic response was observed with direct catalysis of *Dd*FDH on the carbon electrode.[42] These findings have motivated for more extensive investigation of *Dd*FDH with CO_2 in direct and mediated type catalysis. There are still challenges in using enzymes for the process which should be addressed, mainly retaining their stability and electroactivity upon immobilization onto electrodes.[48] Some of the limitations can be overcome using a classical approach of mediated electrochemistry. For this process to be efficient, the correct match between the enzymes and the redox mediators must be carefully assessed.

In this study, *Dd*FDH was electrochemically characterized using a pyrolytic graphite electrode (PGE) to investigate the redox cofactors and their catalytic behavior toward formate and CO_2 in DET regime. In cases where not all *Dd*FDH molecules are properly oriented with the electrode active site (or toward the pathway for the catalytic center) and the electron transfer rate is too low, the scope of electrocatalytic studies was extended in search of a more suitable mediated redox partner. Artificial and natural redox mediators were explored to enhance the catalytic potential of *Dd*FDH. Standard artificial mediators like methyl and benzyl viologens were employed. Additionally, assays with natural physiological partners were conducted through electrocatalytic studies of *Dd*FDH mediated by small electron transfer proteins such as cytochromes. Physiologically, the role of the cytochromes is the transport of electrons between the enzyme's cofactor and its redox partner. In mediated electrocatalysis, this can facilitate the transfer of electrons between redox enzymes and electrodes, establishing an efficient connection between the two.[49,50] In this context, three previously isolated cytochromes from the same organism namely, di-heme cytochrome split-soret (*cyt* SS),[51] tetraheme cytochrome c_3 (*cyt* c_3),[5,2] and monoheme cytochrome c_{552} (*cyt* c_{552})[53] have been electrochemically characterized and used as the mediators to explore *Dd*FDH catalytic activity toward both formate oxidation and CO_2 reduction.

2. Results and Discussion

The experiments were performed either by DET or MET using experimental conditions described below. It was used a PGE designated as *Dd*FDH/PGE and *Dd*FDH/Med/PGE, respectively (**Scheme 1**).

2.1. Electrochemical Characterization of *Dd*FDH

Cyclic voltammetry (CV) was performed at different scan rates to determine the electrochemical behavior of *Dd*FDH on a PGE surface, immobilized with a cellulose membrane (cut-off of 3.5 kDa) in a mixed buffer (100 mM phosphate/acetate buffers, pH = 7). At 10 mV s^{-1}, a broad current wave is observed at −195 mV on the positive direction scan with I_{pa} = 26 nA and at −351 mV on the reverse scan with I_{pc} = −29 nA, resulting in a peak separation (ΔE_p) of 156 mV. The broadness of this peak can be attributed to contributions from the Mo(V/IV) redox couple and the [4Fe–4S] clusters, indicating a quasireversible process, considering at least a two-electron transfer process (calculated number of electrons transferred, n ≈2.6) with a midpoint potential of −273 mV versus NHE (**Figure 1**a). Additionally, the enzyme was immobilized on a membrane, forming a thin enzyme layer on the electrode surface. This approach implies interaction of the enzyme with the electrode without any specific orientation, enabling more redox cofactors to transfer electrons to the electrode surface, contributing to the broadening of the signal. Furthermore, when lower scans were applied, more redox processes can be discriminated. For instance, at 0.5 mV s^{-1} (Figure 1b), four processes with midpoint potentials −170, −210, −317, and −376 mV were observed. As the enzyme contains eight metal cofactors in addition to the Mo-active site, the observed processes result from the overlapping of redox processes. Two weak signals were detected with midpoint potentials at −210 and −170 mV (Processes II and I in Figure 1b, respectively). Three high-potential hemes and the Mo(VI/V) redox

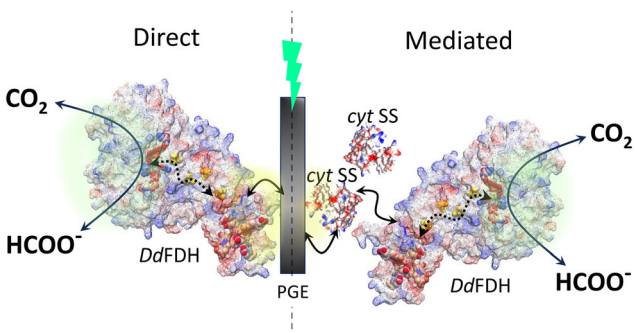

Scheme 1. Illustration of nonmediated and MET with *Dd*FDH (*cyt* SS is used as an example for MET). Surface charge distribution image of Alphafold2[59] predicted structures of *Dd*FDH and *cyt* SS are shown (see also Figure S1, Supporting Information).

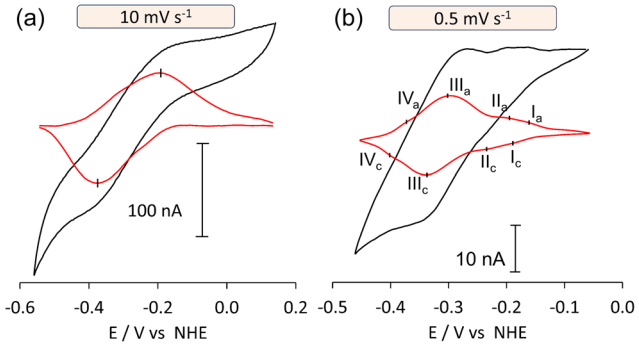

Figure 1. Cyclic voltametric response of *Dd*FDH at higher and lower scan rate in 100 mM mix buffer (acetate/ phosphate) with 100 mM NaCl at pH = 7; black: original and red: baseline subtracted; a) at 10 mV s^{-1} scan and b) at 0.5 mV s^{-1} with assigned four (I, II, III, IV) cathodic and anodic processes with midpoint potentials −170, −210, −317 and −376 mV respectively. The results indicated that lower scan rates are preferable for obtaining better-defined redox processes in the voltammogram. *Dd*FDH amount in each assay = 30 pmol.

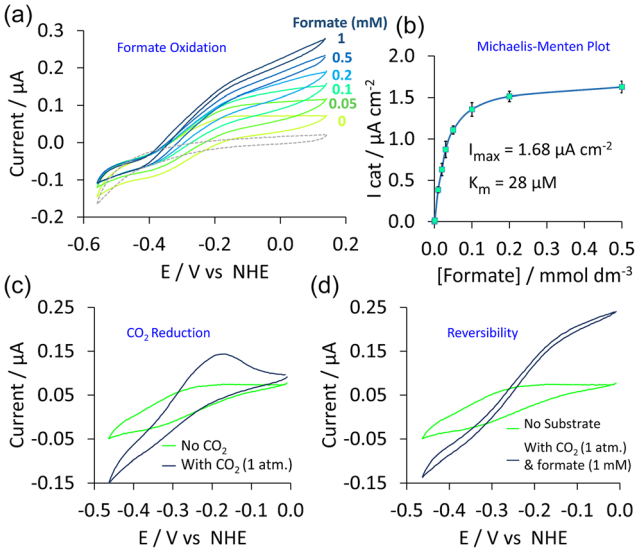

Figure 2. Catalytic voltammograms showing *Dd*FDH/PGE activity in 100 mM mix buffer (acetate/ phosphate) with 100 mM NaCl at pH = 7 a) toward formate oxidation: electrocatalysis with different formate concentration (0 to 1 mM) at pH = 7 at 10 mV s^{-1} scan; dotted line shows the control electrode without enzyme; b) Michaelis–Menten behavior of *Dd*FDH for formate oxidation reaction is shown; c) toward CO_2 reduction: catalytic cathodic current was observed in CO_2-saturated electrolyte (1 atm) at 5 mV s^{-1} scan; d) Reversible CO_2 reduction and formate oxidation attained together in CO_2-saturated (1 atm) electrolyte with 1 mM sodium formate at 5 mV s^{-1} scan. *Dd*FDH amount in each assay = 30 pmol; Current densities were calculated based on the geometric surface area of the electrode of 0.1257 cm^2.

couple are expected to appear within this potential range, as previously described.[43] The Mo(V/IV) redox couple and the four [4Fe–4S] centers, which exhibit closely aligned redox potentials,[42,43] give rise to a broad signal with a midpoint potential of −317 mV (Process III in Figure 1b), characterized by an anodic peak current (Ip_a) of 3.3 nA and a cathodic peak current (Ip_c) of −4.3 nA. The small signal at −376 mV (Process IV in Figure 1b) is attributed to a low-potential heme center.[43]

2.2. Direct *Dd*FDH Electrocatalytic Activity

In **Figure 2**, direct electrocatalytic activities of *Dd*FDH immobilized on pyrolytic graphitic electrode (PGE), termed as *Dd*FDH/PGE, toward formate oxidation as well as CO_2 reduction were accomplished by CV. Addition of formate resulted in the increase of the anodic current, consistent with expected enzymatic activity as formate is being oxidized to CO_2 and consequently an increased reduced species in the enzyme center ready to be oxidized (Figure 2a). This increase in current density follows saturation kinetics with current density 1.68 µA cm^{-2} at +140 mV and Michaelis–Menten constant K_m = 28 µM (Figure 2b). Cathodic current for CO_2 reduction was also observed when CO_2 was purged directly into the electrolyte with a maximum current density of 1.20 µA cm^{-2} at −460 mV (Figure 2c). The addition of formate into CO_2-saturated electrolyte enabled reversible interconversion of CO_2 and formate with a characteristic sigmoidal shape (Figure 2d).

2.3. Mediated *Dd*FDH Electrocatalytic Activity with Artificial Redox Partners

Mediated catalytic activity was explored with standard artificial redox mediators, such as viologens, which are a class of organic molecules containing negative redox potential around the range −300 to −450 mV. These compounds present well-defined redox processes, making them suitable as mediators for the study of redox enzymes. Methyl viologen (MV) and benzyl viologen (BV) are two such conventional viologens in the lowest and highest redox potential region, respectively, in the viologen family.[54] CV experiments were performed with the dichloride salts of 0.5 mM MV or BV in the electrolyte (100 mM mix buffer with 100 mM NaCl at pH = 7) at 10 mV s^{-1} and the midpoint potentials were obtained as −455 and −296 mV, respectively (see Figure S2, Supporting Information). In mediated electrocatalysis, anodic current densities for formate oxidation reach up to 60 µA cm^{-2} at −320 mV with MV and 58 µA cm^{-2} at −220 mV with BV, which are comparative (**Figure 3**a,b). Moreover, MV-mediated CO_2 reduction reaction shows high efficiency and the cathodic current reaches 216 µA cm^{-2} at −560 mV. Whereas, in comparison, BV-mediated CO_2 reduction presents the maximum current density of 22 µA cm^{-2} at −480 mV. Both the viologens showed mediating ability for formate oxidation. However, only MV has been shown to be a highly efficient mediator for the CO_2 reduction reaction, likely due to its lower formal reduction potential (−445 mV) with respect to the reported *Dd*FDH potentials.[42]

2.4. *Dd*FDH Activity Toward Formate Oxidation Detected Spectrophotometrically: Role of cyt SS as Redox Partner

Catalytic activity of *Dd*FDH was observed spectrophotometrically by following the reduction of the external electron acceptor, BV, at 555 nm. An assay of *Dd*FDH, incubated for 30 min with formate and DTT under argon atmosphere, and the reaction was started with the addition of 7.5 mM BV, was found to have high efficiency toward formate oxidation with a specific activity of 243 mU $µg^{-1}$ (**Figure 4**a). Small electron transfer protein, such as cytochrome

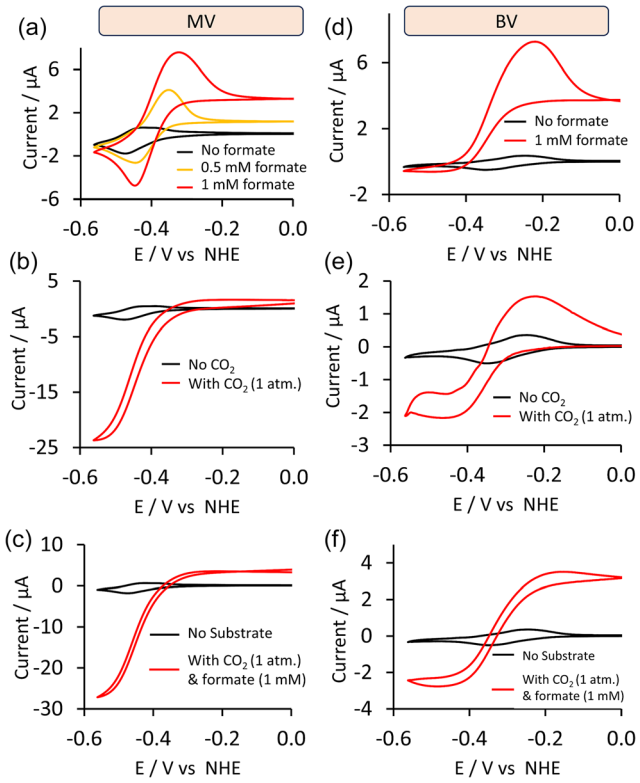

Figure 3. Mediated catalytic voltammogram: a–c) *Dd*FDH/MV/PGE activity with 0.5 mM MV showing, (a) formate oxidation in presence of 0 to 1 mM formate added to electrolyte (b) CO_2 reduction in CO_2-saturated (1 atm) electrolyte (c) Reversible CO_2 reduction and formate oxidation attained together in CO_2-saturated (1 atm) electrolyte with 1 mM sodium formate; d–f) *Dd*FDH/BV/PGE activity with 0.5 mM BV showing, (d) formate oxidation in presence of 0 to 1 mM formate added to electrolyte (e) CO_2 reduction in CO_2-saturated (1 atm) electrolyte (f) Reversible CO_2 reduction and formate oxidation attained together in CO_2-saturated (1 atm) electrolyte with 1 mM sodium formate. *Dd*FDH amount in each assay = 30 pmol.

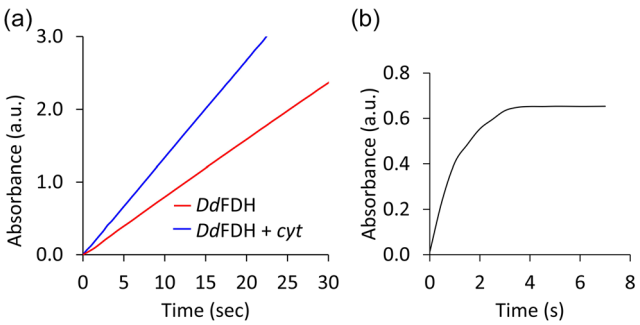

Figure 4. *Dd*FDH catalyzed formate oxidation activity assays: a) Representative time courses of 6 nM *Dd*FDH (red) and 6 nM *Dd*FDH with 12 µM *cyt* SS (blue) in 10 mM formate and 0.5 mM DTT were incubated for 30 min under argon bubble. The reaction was started with 7.5 mM benzyl viologen and followed through reduction of viologen at 555 nm; b) Role of *cyt* SS as a redox partner: Time course of 6 nM *Dd*FDH with 10 mM formate and 0.5 mM DTT was incubated for 30 min under an Argon bubble. The reaction was started with 6 µM *cyt* SS and reduction of heme was followed at 552 nm.

split-soret (*cyt* SS), was thought to be a potential candidate for the physiological partner of *Dd*FDH. In that case, *cyt* SS would interact with *Dd*FDH to improve its activity. To test that, at first, *cyt* SS was added into the *Dd*FDH activity assay at a lower concentration (6 nM *Dd*FDH: 24 nM *cyt* SS) with no significant increment in activity. Addition of *cyt* SS at an excess concentration (6 nM *Dd*FDH: 12 µM *cyt* SS) has improved the activity, resulting in around a 1.7 times increase in the specific activity to 413 mU μg^{-1} (Figure 4a).

The role of *cyt* SS was also explored as a redox partner of *Dd*FDH, replacing BV in the presence of formate. The reduction was followed spectrophotometrically by the appearance of the α-band of reduced *cyt* SS at 552 nm. In this condition, similar activity assays were performed where *Dd*FDH was incubated for 30 min with formate and DTT under an argon atmosphere, but the reaction was started with the addition of 6 µM of *cyt* SS instead of BV. With *cyt* SS as a partner, *Dd*FDH was observed to have specific activity of 83 mU μg^{-1} (Figure 4b). Corresponding control assays were performed without *Dd*FDH, and no reduction of *cyt* SS was found (see Figure S3, Supporting Information) nor formate oxidation. Thus, a small electron transfer protein like *cyt* SS can be used as an efficient mediator for the catalysis with *Dd*FDH.

2.5. Electrochemical Characterization of Small Electron Carrier Proteins (Cytochromes)

The *c*-type cytochromes belong to the family of small hemoproteins containing single or multiple heme groups, which are covalently bound to the apoprotein through a thioether bond with cystine residues. Three of such previously isolated *c*-type cytochromes, di-heme cytochrome split-soret (*cyt* SS),[51,55] tetraheme cytochrome c_3 (*cyt* c_3),[52,56] and monoheme cytochrome c_{552} (*cyt* c_{552})[53] from the same microbe were immobilized within a cellulose membrane on a PGE carbon electrode (thin-layer configuration) and characterized to determine the midpoint potentials at pH = 7. Both *cyt* SS and *cyt* c_3 have shown a broad single couple at 10 mV s^{-1} (see Figure S4, Supporting Information). However, at a very low scan rate (1 mV s^{-1}), different redox couples were observed and were assigned to the individual hemes. The *cyt* SS displays two distinct redox couples at midpoint potentials −164 mV and at −325 mV (**Figure 5**a), which are in agreement with previously calculated potential values.[42] Similarly, in *cyt* c_3, three well-defined couples were observed with midpoint potentials of −130, −227, and −338 mV (Figure 5b).[57] The difference in midpoint potentials of the main process(es) of the different cytochromes should be highlighted, in particular the monoheme *cyt* c_{552} exhibiting a midpoint potential of +21 mV (Figure 5c). All of the cytochromes exhibit quasireversible behavior as expected for this type of redox protein.

2.6. Mediated *Dd*FDH Electrocatalytic Activity with Small Electron Transfer Proteins

Small redox proteins are considered good mediators for sulfate-reducing organisms, such as *Dd*FDH exchanging electrons with their physiological partners.[58] In search of *Dd*FDH's physiological partner, the interaction of such small electron transfer proteins with *Dd*FDH was explored. Electrocatalytic activity of *Dd*FDH co-immobilized with either of three individual cytochromes (2 µl of 15 µM *Dd*FDH with 6 µl 120 µM cytochrome ≡ [*cyt c*]/[*Dd*FDH] = 24 times), termed as *Dd*FDH/*cyt c*/PGE, was studied

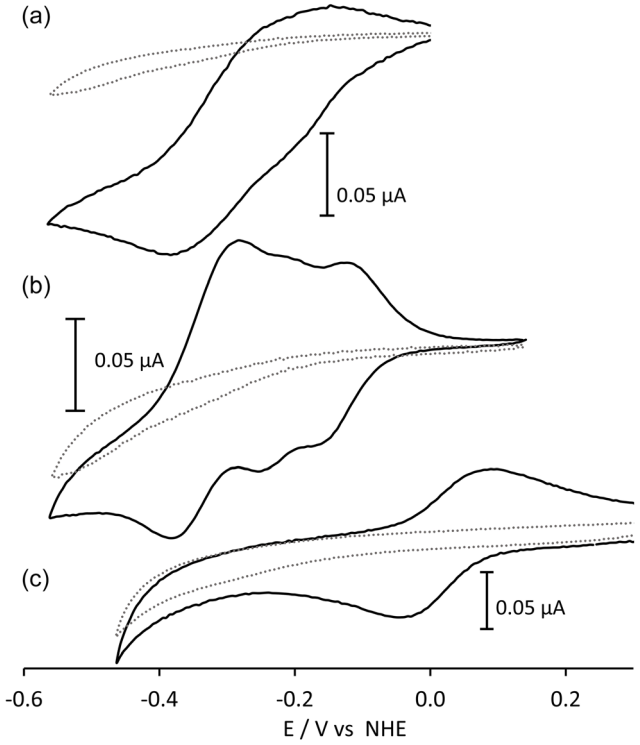

Figure 5. Voltammograms of *c*-type cytochromes with the respective control (absence of protein) CV in 100 mM mix buffer (acetate/ phosphate) with 100 mM NaCl at pH = 7; a) *cyt* SS at 1 mV s^{-1}, b) *cyt* c_3 at 1 mV s^{-1}; c) *cyt* c_{552} at 5 mV s^{-1} scan.

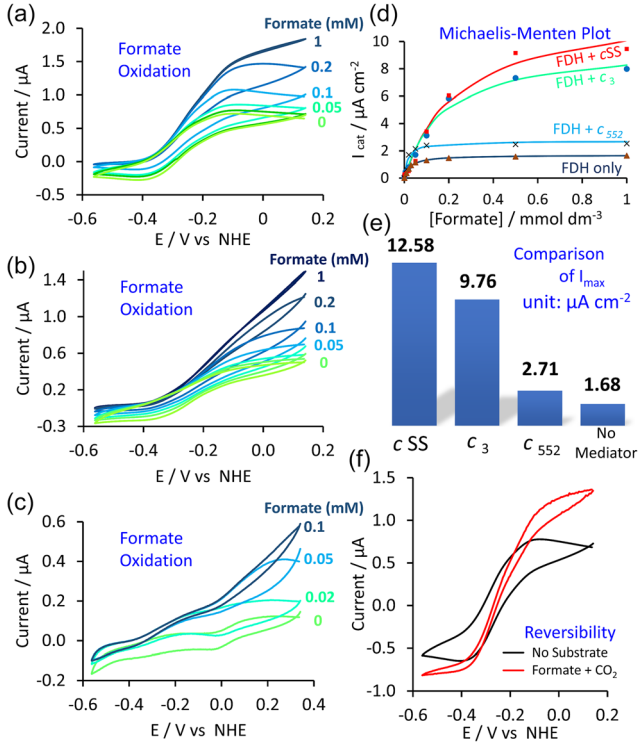

Figure 6. a–c) Catalytic voltammogram showing the *Dd*FDH/*cyt c*/PGE activity toward formate oxidation at 10 mV s^{-1} rate in different formate concentration (0 to 1 mM) in 100 mM mix buffer (acetate/ phosphate) with 100 mM NaCl at pH = 7, (a) *cyt* SS; (b) *cyt* c_3; (c) *cyt* c_{552}; d) Michaelis–Menten behavior of *Dd*FDH with three cytochromes mediated formate oxidation reaction is shown; e) comparison of maximum catalytic current density of direct and mediated reactions is compared; f) CV of *Dd*FDH/*cyt* SS/PGE activity: reversible CO_2 reduction and formate oxidation attained together in CO_2-saturated (1 atm) electrolyte with 1 mM sodium formate at 10 mV s^{-1} scan. *Dd*FDH amount in each assay = 30 pmol; Current densities were calculated based on the geometric surface area of the electrode of 0.1257 cm^2.

and compared. In each of the cases, an increase in anodic current with formate addition was observed, following the saturation kinetics (**Figure 6**d), and their maximum current density was compared with the one attained by direct catalysis (Figure 6e). However, corresponding control experiments were performed with all three individual cytochromes in the same conditions, and no catalytic current was observed (see Figure S4, Supporting Information). Mediated catalysis with *cyt* SS, in the presence of increasing formate concentration, has shown a significant increment in anodic current (Figure 6a). Maximum catalytic current density achieved for formate oxidation mediated by *cyt* SS was found to be 12.58 μA cm^{-2}, which is around 7.5 times higher than direct catalysis. Mediated catalysis with *cyt* c_3 also shows similar behavior with a current density of 8.76 μA cm^{-2} (Figure 6b). However, the monoheme *cyt* c_{552} was not found to be a good mediator for electrocatalytic reactions of *Dd*FDH with maximum current density close to the nonmediated one (Figure 6c).

Reversibility of *cyt* SS-mediated catalytic reaction (*Dd*FDH/*cyt* SS/PGE) with both CO_2 and formate into the electrolyte was also studied, as *cyt* SS was demonstrated as a better mediator than the other two. Figure 6f displays an increase in both cathodic and anodic current in the presence of both substrates, proving such reversible nature of *Dd*FDH in mediated conditions. Moreover, the dependence of *cyt* SS in the mediated electrocatalysis for *Dd*FDH/*cyt* SS/PGE was tested. The current was found to be increasing with *cyt* SS concentration with respect to *Dd*FDH, where the [*cyt* SS]/[*Dd*FDH] concentration ratio was studied up to 40 times (see Figure S5, Supporting Information).

A comparative table (Table S1, Supporting Information) has been added summarizing some similar CO_2 reduction results with metal-dependent and metal-independent FDHs in direct and mediated catalytic conditions. The overall result achieved in this work, through MV-mediated catalysis with *Dd*FDH, is among the highest CO_2 reduction currents achieved while utilizing the lowest amount of *Dd*FDH enzyme (30 pmol) among comparable studies. However, the current observed for direct electrocatalysis was significantly lower than that for mediated catalysis. This may be attributed to the limited number of available electroactive enzyme molecules properly oriented on the electrode surface. This suggests that there is room for improvement by exploring alternative electrode materials, such as porous carbons or metal oxides, and optimizing reaction conditions where *Dd*FDH could be immobilized efficiently with favorable orientation, facilitating DET, ensuring its durability and electrocatalytic performance is maintained. Furthermore, as frequently discussed, a comparison of the electrochemical behavior of metal-dependent and metal-independent FDHs reveals slight differences. In this study, such distinctions can be observed between *Dd*FDH and *Cb*FDH[28] as expected. For instance, regarding the reversibility under noncatalytic conditions, *Dd*FDH exhibited a quasireversible process

with a broader peak separation, which is a typical characteristic for metalloproteins with multiple redox cofactors. In comparison, *Cb*FDH showed reversible electrochemical behavior.[28] Moreover, in catalytic conditions, the direct electrocatalysis of *Dd*FDH/PGE seems apparently to be more irreversible compared to the results shown by Su et al. using *Cb*FDH.[28] In addition to the differences in experimental conditions and the type of enzymes used, there are other factors that contribute to the observed behavior variations. Firstly, it is important to note that even in the referenced study[28] regarding *Cb*FDH the electrochemical reversibility is not complete, as evidenced by a more pronounced cathodic process compared to the anodic one. However, both processes exhibit a typical mass-controlled (bell) shape, far from the limiting current. In our study with *Dd*FDH/PGE, under catalytic conditions and at lower scan rates, the current features deviate from being solely diffusion-controlled and become increasingly governed by charge transfer, resulting in a limiting current. Consequently, the redox potentials of the FDH centers are no longer discernible, giving the appearance of partial irreversibility. With further decreases in scan rate, charge-transfer control becomes more dominant, whereas at higher scan rates, the process reverts to being primarily diffusion-controlled.

Furthermore, *Dd*FDH has also demonstrated exceptional robustness as an electrocatalyst operating efficiently in aqueous medium under very mild, ambient conditions during the experiments in both direct and mediated regimes, while it maintained most of its activity even after 24 h (data not shown) and in the presence of oxygen. This highlights *Dd*FDH's potential as a prime candidate for integration into BES. Building on this observation, the next step is to incorporate it heterogeneously into a porous medium.

3. Conclusion

To conclude, *Dd*FDH and three native *c*-type cytochromes were electrochemically characterized on a PGE. Cyclic voltammograms at low scan rates enable us to look into multiple redox processes, allowing us to determine the redox potentials of individual redox cofactors present within. Further, direct catalytic activity of *Dd*FDH was studied to achieve a current density of 1.68 $\mu A\,cm^{-2}$ following Michaelis–Menten kinetics with Km = 28 μM for formate oxidation and a current density of 1.20 $\mu A\,cm^{-2}$ for CO_2 reduction. *Dd*FDH also shows reversibility in the presence of both substrates, enabling the interconversion of formate and CO_2. Furthermore, mediated electrocatalysis using viologens and potential physiological redox partners was observed at a faster rate. Both MV and BV showed mediating activity toward formate oxidation. However, MV, having a lower redox potential than BV and *Dd*FDH, acts as an efficient mediator for CO_2 reduction, achieving a very high current density of 216 $\mu A\,cm^{-2}$. In search of the physiological mediator, small electron transfer proteins were electrochemically characterized at low scan rates, which allowed the study of their individual hemes. The cytochromes mediated catalysis have shown an improved catalytic activity following Michaelis–Menten behavior. Catalytic activity using cytochrome-mediated reactions revealed a 7.5 times increase for *cyt* SS and a 5.8 times increase for *cyt* c_3 and an insignificant amount of increase for *cyt* c_{552}, which makes *cyt* SS the most efficient redox mediator among the cytochromes, in line with the hypothesis of this species being the natural partner of *Dd*FDH. In this study, our primary focus was to explore electrocatalytic conditions for *Dd*FDH and to identify a suitable mediator. However, its scope of applicability on an industrial scale remains in the very early stages. It is still a significant challenge to ensure the long-term stability of *Dd*FDH on a solid electrode support while maintaining its activity at elevated temperatures. Further studies on electrocatalytic activity toward CO_2 are underway to optimize these experimental conditions.

Acknowledgements

This work was supported by the PTDC/BTA-BTA/0935/2020 project and by the Associate Laboratory for Green Chemistry-LAQV (UID/50006/2023), which are financed by national funds from Fundação para a Ciência e a Tecnologia, MCTES (FCT/MCTES).

Conflict of Interest

The authors declare no conflict of interest.

Data Availability Statement

The data that support the findings of this study are available from the corresponding author upon reasonable request.

Keywords: bioelectrochemistry · CO_2 reductions · cytochromes · enzymatic activities · formate dehydrogenases

[1] P. Friedlingstein, M. O. Sullivan, M. W. Jones, R. M. Andrew, D. C. E. Bakker, J. Hauck, P. Landschützer, C. Le Quéré, I. T. Luijkx, G. P. Peters, W. Peters, J. Pongratz, C. Schwingshackl, S. Sitch, J. G. Canadell, P. Ciais, R. B. Jackson, S. R. Alin, P. Anthoni, L. Barbero, N. R. Bates, M. Becker, N. Bellouin, B. Decharme, L. Bopp, I. B. M. Brasika, P. Cadule, M. A. Chamberlain, N. Chandra, et al., *Earth Syst. Sci. Data* **2023**, *15*, 5301.
[2] H. S. Baker, R. J. Millar, D. J. Karoly, U. Beyerle, B. P. Guillod, D. Mitchell, H. Shiogama, S. Sparrow, T. Woollings, M. R. Allen, *Nat. Clim. Change* **2018**, *8*, 604.
[3] A. M. Appel, J. E. Bercaw, A. B. Bocarsly, H. Dobbek, D. L. DuBois, M. Dupuis, J. G. Ferry, E. Fujita, R. Hille, P. J. A. Kenis, C. A. Kerfeld, R. H. Morris, C. H. F. Peden, A. R. Portis, S. W. Ragsdale, T. B. Rauchfuss, J. N. H. Reek, L. C. Seefeldt, R. K. Thauer, G. L. Waldrop, *Chem. Rev.* **2013**, *113*, 6621.
[4] M. Aresta, A. Dibenedetto, A. Angelini, *Chem. Rev.* **2014**, *114*, 1709.
[5] O. S. Bushuyev, P. De Luna, C. T. Dinh, L. Tao, G. Saur, J. van de Lagemaat, S. O. Kelley, E. H. Sargent, *Joule* **2018**, *2*, 825.
[6] Y. Hori, in *Modern Aspects of Electrochemistry* (Eds: C. G. Vayenas, R. E. White, M. E. Gamboa-Aldeco), Springer New York, New York, NY **2008**, pp. 89–189.
[7] C. Costentin, M. Robert, J.-M. Savéant, *Chem. Soc. Rev.* **2013**, *42*, 2423.
[8] L. B. Maia, I. Moura, J. J. G. Moura, in *Enzymes for Solving Humankind's Problems: Natural and Artificial Systems in Health, Agriculture, Environment and Energy* (Eds: J. J. G. Moura, I. Moura, L. B. Maia), Springer International Publishing, Cham **2021**, pp. 29–81.
[9] M. Meneghello, C. Léger, V. Fourmond, *Chem. Eur. J.* **2021**, *27*, 17542.
[10] K. Kano, *Biosci. Biotechnol. Biochem.* **2021**, *86*, 141.
[11] J. A. Cracknell, K. A. Vincent, F. A. Armstrong, *Chem. Rev.* **2008**, *108*, 2439.
[12] D. Niks, R. Hille, *Protein Sci.* **2019**, *28*, 111.
[13] L. B. Maia, J. J. G. Moura, I. Moura, *J. Biol. Inorg. Chem.* **2015**, *20*, 287.

[14] L. B. Maia, I. Moura, J. J. G. Moura, in *Molybdenum and Tungsten Enzymes: Biochemistry*, The Royal Society of Chemistry, Cambridge **2017**, pp. 1–80.
[15] C. M. Cordas, J. J. G. Moura, A. Escapa, R. Mateos, in *Enzymes for Solving Humankind's Problems: Natural and Artificial Systems in Health, Agriculture, Environment and Energy* (Eds: J. J. G. Moura, I. Moura, L. B. Maia), Springer International Publishing, Cham **2021**, pp. 83–108.
[16] V. O. Popov, V. S. Lamzin, *Biochem. J.* **1994**, *301*, 625.
[17] Q. Guo, L. Gakhar, K. Wickersham, K. Francis, A. Vardi-Kilshtain, D. T. Major, C. M. Cheatum, A. Kohen, *Biochemistry* **2016**, *55*, 2760.
[18] S. Alpdağtaş, O. Turunen, J. Valjakka, B. Binay, *Crit. Rev. Biotechnol.* **2022**, *42*, 953.
[19] R. Sato, Y. Amao, *New J. Chem.* **2020**, *44*, 11922.
[20] W. A. van der Donk, H. Zhao, *Curr. Opin. Biotechnol.* **2003**, *14*, 421.
[21] G. Liu, H. Chen, H. Zhao, R. Chen, M. Yang, J. Gao, F. Yu, Y. Jiang, *ACS Sustain. Chem. Eng.* **2022**, *10*, 633.
[22] S. Kim, M. K. Kim, S. H. Lee, S. Yoon, K.-D. Jung, *J. Mol. Catal. B Enzym.* **2014**, *102*, 9.
[23] N. Hernández-Ibáñez, A. Gomis-Berenguer, V. Montiel, C. O. Ania, J. Iniesta, *Chemosphere* **2022**, *291*, 133117.
[24] A. Tülek, E. Günay, B. Servili, S. Essiz, B. Binay, D. Yildirim, *Sep. Purif. Technol.* **2023**, *309*, 123090.
[25] M. M. Çakar, J. Ruupunen, J. Mangas-Sanchez, W. R. Birmingham, D. Yildirim, O. Turunen, N. J. Turner, J. Valjakka, B. Binay, *Biotechnol. Lett.* **2020**, *42*, 2251.
[26] J. Meyer, M. Romero, J. Thöming, M. Baune, N. Reimer, R. Dringen, I. Bösing, *Sci. Rep.* **2023**, *13*, 22394.
[27] B. S. Jayathilake, S. Bhattacharya, N. Vaidehi, S. R. Narayanan, *Acc. Chem. Res.* **2019**, *52*, 676.
[28] Z. Su, R. Elmahdy, J. F. Biernat, A. Chen, J. Lipkowski, *Langmuir* **2024**, *40*, 16249.
[29] T. Reda, C. M. Plugge, N. J. Abram, J. Hirst, *Proc. Natl. Acad. Sci.* **2008**, *105*, 10654.
[30] V. M. Badiani, C. Casadevall, M. Miller, S. J. Cobb, R. R. Manuel, I. A. C. Pereira, E. Reisner, *J. Am. Chem. Soc.* **2022**, *144*, 14207.
[31] J. Alvarez-Malmagro, A. R. Oliveira, C. Gutiérrez-Sánchez, B. Villajos, I. A. C. Pereira, M. Vélez, M. Pita, A. L. De Lacey, *ACS Appl. Mater. Interfaces* **2021**, *13*, 11891.
[32] K. Sakai, Y. Sugimoto, Y. Kitazumi, O. Shirai, K. Takagi, K. Kano, *Electrochim. Acta* **2017**, *228*, 537.
[33] M. Miller, W. E. Robinson, A. R. Oliveira, N. Heidary, N. Kornienko, J. Warnan, I. A. C. Pereira, E. Reisner, *Angew. Chem. Int. Ed.* **2019**, *58*, 4601.
[34] W. Li, Y. Gao, X. Sun, L. Wan, H. Ji, H. Luo, Y. Tian, H. Song, G. Wu, L. Zhang, *Carbon Energy* **2023**, *5*, e304.
[35] S. K. Kuk, K. Gopinath, R. K. Singh, T.-D. Kim, Y. Lee, W. S. Choi, J.-K. Lee, C. B. Park, *ACS Catal.* **2019**, *9*, 5584.
[36] K. Sakai, Y. Kitazumi, O. Shirai, K. Kano, *Electrochem. Commun.* **2016**, *65*, 31.
[37] M. Yuan, S. Sahin, R. Cai, S. Abdellaoui, D. P. Hickey, S. D. Minteer, R. D. Milton, *Angew. Chem., Int. Ed. Engl.* **2018**, *57*, 6582.
[38] J. Szczesny, A. Ruff, A. R. Oliveira, M. Pita, I. A. C. Pereira, A. L. De Lacey, W. Schuhmann, *ACS Energy Lett.* **2020**, *5*, 321.
[39] P. Kalimuthu, S. Hakopian, D. Niks, R. Hille, P. V. Bernhardt, *J. Phys. Chem. B* **2023**, *127*, 8382.
[40] V. P. Hitaishi, R. Clement, N. Bourassin, M. Baaden, A. De Poulpiquet, S. Sacquin-Mora, A. Ciaccafava, E. Lojou, *Catalysts* **2018**, *8*, 192.
[41] L. B. Maia, L. Fonseca, I. Moura, J. J. G. Moura, *J. Am. Chem. Soc.* **2016**, *138*, 8834.
[42] C. M. Cordas, M. Campaniço, R. Baptista, L. B. Maia, I. Moura, J. J. G. Moura, *J. Inorg. Biochem.* **2019**, *196*, 110694.
[43] C. Costa, M. Teixeira, J. LeGall, J. J. G. Moura, I. Moura, *J. Biol. Inorg. Chem.* **1997**, *2*, 198.
[44] M. G. Rivas, P. J. González, C. D. Brondino, J. J. G. Moura, I. Moura, *J. Inorg. Biochem.* **2007**, *101*, 1617.
[45] D. Niks, J. Duvvuru, M. Escalona, R. Hille, *J. Biol. Chem.* **2016**, *291*, 1162.
[46] T. Yoshikawa, F. Makino, T. Miyata, Y. Suzuki, H. Tanaka, K. Namba, K. Kano, K. Sowa, Y. Kitazumi, O. Shirai, *Chem. Commun.* **2022**, *58*, 6478.
[47] C. Léger, P. Bertrand, *Chem. Rev.* **2008**, *108*, 2379.
[48] N. D. J. Yates, M. A. Fascione, A. Parkin, *Chem. Eur. J.* **2018**, *24*, 12164.
[49] S. Ma, R. Ludwig, *ChemElectroChem* **2019**, *6*, 958.
[50] H. Lopes, S. Besson, I. Moura, J. J. G. Moura, *J. Biol. Inorg. Chem.* **2001**, *6*, 55.
[51] B. Devreese, C. Costa, H. Demol, V. Papaefthymiou, I. Moura, J. J. R. Moura, J. Van Beeumen, *Eur. J. Biochem.* **1997**, *248*, 445.
[52] I. Moura, G. Fauque, J. LeGall, A. V. Xavier, J. J. G. Moura, *Eur. J. Biochem.* **1987**, *162*, 547.
[53] C. Costa, PhD Thesis, Universidade NOVA De Lisboa (PT) **1994**.
[54] D. A. Koomson, J. H. Nicholson, A. P. S. Brogan, L. Aldous, *Chem. Sci.* **2024**, *15*, 9325.
[55] J. J. Moura, C. Costa, M. Y. Liu, I. Moura, J. LeGall, *Biochim. Biophys. Acta* **1991**, *1058*, 61.
[56] T. Yagi, K. Maruyama, *Biochim. Biophys. Acta, Protein Struct.* **1971**, *243*, 214.
[57] D. E. Stewart, J. LeGall, I. Moura, J. J. G. Moura, H. D. Peck Jr, A. V. Xavier, P. K. Weiner, J. E. Wampler, *Eur. J. Biochem.* **1989**, *185*, 695.
[58] G. R. Bell, J.-P. Lee, H. D. Peck, J. Le Gall, *Biochim.* **1978**, *60*, 315.
[59] J. Jumper, R. Evans, A. Pritzel, T. Green, M. Figurnov, O. Ronneberger, K. Tunyasuvunakool, R. Bates, A. Žídek, A. Potapenko, A. C. Meyer, S. A. A. Kohl, A. J. Ballard, A. Cowie, B. Romera-Paredes, S. Nikolov, R. Jain, J. Adler, T. Back, S. Petersen, D. Reiman, E. Clancy, M. Zielinski, M. Steinegger, M. Pacholska, T. Berghammer, S. Bodenstein, D. Silver, O. Vinyals, et al., *Nature* **2021**, *596*, 583.

Manuscript received: March 25, 2025
Revised manuscript received: May 23, 2025
Version of record online: June 12, 2025